

Spatio-temporal dynamics of bumblebees foraging under predation risk

Friedrich Lenz,¹ Thomas C. Ings,² Lars Chittka,² Aleksei V. Chechkin,³ and Rainer Klages^{1,*}

¹*School of Mathematical Sciences, Queen Mary University of London, Mile End Road, London E1 4NS, UK*

²*School of Biological and Chemical Sciences, Queen Mary University of London, Mile End Road, London E1 4NS, UK*

³*Institute for Theoretical Physics, NSC KIPT, ul. Akademicheskaya 1, UA-61108 Kharkov, Ukraine*

We study bumblebees searching for nectar in a laboratory experiment with and without different types of artificial spiders as predators. We find that the flight velocities obey mixed probability distributions reflecting the access to the food sources while the threat posed by the spiders shows up only in the velocity correlations. This means that the bumblebees adjust their flight patterns spatially to the environment and temporally to the predation risk. Key information on response to environmental changes is thus contained in temporal correlation functions and not in spatial distributions.

PACS numbers: 87.10.-e, 87.19.lv, 05.40.Fb

Quantifying foraging behavior of organisms by statistical analysis has raised the question whether biologically relevant search strategies can be identified by mathematical modeling [1–6]. For sparsely, randomly distributed, replenishing food sources, the Lévy flight hypothesis predicts that a random search with jump lengths following a power law minimizes the search time [7, 8]. Experimental evidence [9–12] and further theoretical analyses [13, 14] supporting this hypothesis were challenged by refined statistical data analyses [15–18] and more detailed theoretical modeling [6, 19, 20]. A crucial problem is how dispositions of a forager like memory [21] or sensory perception [22], as well as properties of the environment [11, 12, 23–25], can be tested in a statistical foraging analysis [1–3, 5]. Especially for data obtained from foraging experiments in the wild, it is typically not clear to which extent extracted search patterns are determined by forager dispositions, or reflect an adjustment of the dynamics of organisms to the distribution of food sources and the presence of predators [5, 11, 12]. This problem can be addressed by statistically quantifying search behavior in laboratory experiments where foraging conditions are varied in a fully controlled manner [12, 23]. Such an experiment has recently been performed by Ings and Chittka [26, 27], who studied the foraging behavior of bumblebees with and without different types of artificial spiders mimicking predators.

In this Letter we ask the question whether changes of environmental conditions as performed in the experiment by Ings and Chittka lead to changes in the foraging process. We answer this question by a statistical physical analysis of the bumblebee flights recorded in this experiment on both spatial and temporal scales. For this purpose, we extract both flight velocity probability distributions and temporal velocity autocorrelation functions from the data. Surprisingly, we find that the crucial quantity to understand the changes of the bumblebee dynamics under variation of the predation risk is not the distribution function, as implied by the Lévy flight hypothesis [7, 8], but the correlation function. In order to construct a theory of the foraging of organisms, our results thus suggest to shift the focus from scale-free models to the statistical quan-

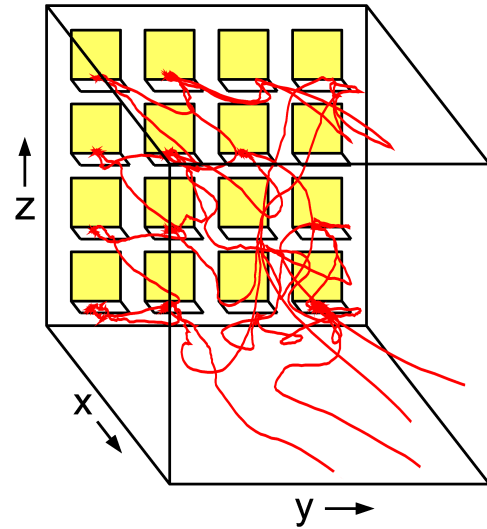


Figure 1. Diagram of the foraging arena together with part of flight trajectory of a single bumblebee. The bumblebees forage on a grid of artificial flowers at one wall of the box. While being on the landing platforms, the bumblebees have access to food supply. All flowers can be equipped with spider models and trapping mechanisms simulating predation attempts.

tification of spatio-temporal changes in the foraging dynamics due to interactions with the environment.

In the experiment [26, 27] bumblebees (*Bombus terrestris*) were flying in a cubic arena of ≈ 75 cm side length by foraging on a 4×4 vertical grid of artificial yellow flowers on one wall. In total the 3D positions of 30 bumblebees, tested sequentially and individually, were tracked by two high frame rate cameras ($\Delta t = 0.02$ s). On the landing platform of each flower, nectar was given to the bumblebees. The short trajectory in Fig. 1 shows typical foraging behavior of a bumblebee. To analyze differences in the foraging behavior of the bumblebees under threat of predation, artificial spiders were introduced.

The experiment was staged into three phases: (1) spider-free foraging, (2) foraging under predation risk and (3) a memory test one day later. Before and directly after stage (2) the bumblebees were trained to forage in the presence of artificial

* r.klages@qmul.ac.uk

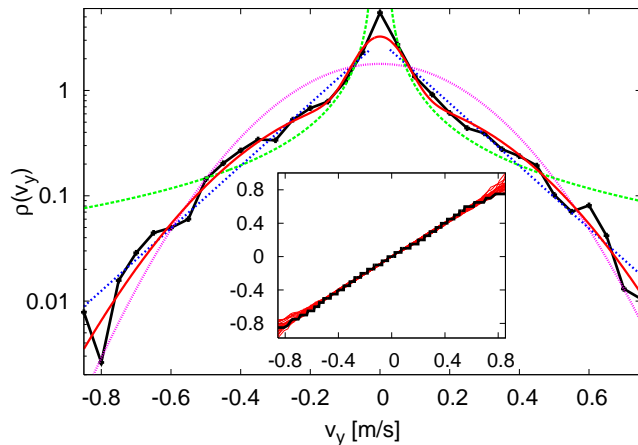


Figure 2. Estimated velocity distributions (main part) and Quantile-Quantile plot of a Gaussian mixture as the best fit (inset). Semi-logarithmic plot of the normalized histogram of velocities v_y parallel to the y -axis in Fig. 1 (black crosses) for a single bumblebee in the spider-free stage (1) together with a Gaussian mixture (red line), exponential (blue dotted), power law (green dashed), and Gaussian distribution (violet dotted), fitted via maximum likelihood estimation. The inset shows quantiles of v_y (in m/s) of a single bumblebee against quantiles of an estimated mixture of two Gaussians. An ideal match would yield a straight line. The dashed red lines show 20 surrogate data sets of the same size.

spiders, which were randomly placed on 25% of the flowers. A spider was emulated by a spider model on the flower and a trapping mechanism which held the bumblebee for two seconds to simulate a predation attempt. In (2) and (3) the spiders models were present but the traps inactive in order to analyze the influence of previous experience with predation risk on the bumblebees' flight dynamics. To see whether the detectability of the spiders is an important factor, half of the bumblebees were trained on easily visible (white) spider models and half of them on yellow models, which make the spiders cryptic on the yellow flowers; see Ings and Chittka [26] for further details of the experiment.

Figure 2 shows a typical normalized histogram of the horizontal velocities parallel to the flower wall (cf. y -direction in Fig. 1) for a single bumblebee. The histograms are characterized by a peak at low velocities and vary in the different spatial directions due to asymmetries induced by physical and biological constraints as well as the spatial arrangement of the flowers. Direct fitting of distributions on the histogram and a visual comparison with some assumed distribution was shown to be unreliable [16], as is illustrated by Fig. 2: only the power law and the Gaussian distribution can be ruled out by visual inspection. However, the Gaussian mixture and an exponential function appear to be equally likely. Therefore we use the maximum likelihood method for a number of candidate distributions to obtain the optimal parameters for each candidate and then compare the different distribution types by their weights using the Akaike information criterion. Our candidate distributions are: (a) Exponential: $\rho_\lambda(v) = ce^{-\lambda|v|}$, (b) Power law: $\rho_\mu(v) = c|v|^{-\mu}$, (c) Normal distribution with

zero mean: $\rho_\sigma(v) = N_\sigma(v)$, (d) Mixture of two normal distributions: $\rho_{a,\sigma_1,\sigma_2}(v) = aN_{\sigma_1}(v) + (1-a)N_{\sigma_2}(v)$, where $N_{\sigma_i}(v) = \frac{1}{\sqrt{2\pi\sigma_i^2}}e^{-\frac{v^2}{2\sigma_i^2}}$, $i = 1, 2$, and $0 \leq a \leq 1$. Details of this analysis are described in the Supplemental Material.

For the data sets of all bumblebees and in all stages of the experiment the Akaike weights show that a mixture of two Gaussians is the preferred distribution of the tested candidates (see Table I in the Supplemental Material). However, they do not inform us if the best of the candidates is actually a good model: if all of the candidates are far off the real distribution, the Akaike weights could highlight one of them as the best of the poor fits. As a supplementary qualitative test to which extent the estimated distribution with the largest Akaike weight deviates from the data over the whole range variables, we use Quantile-Quantile (Q-Q) plots. The inset of Fig. 2 shows the Q-Q plot of the mixture of two Gaussians against the experimental data of a single bumblebee and 20 surrogate data sets. Each of the surrogate data sets consists of independently identically distributed random numbers drawn from the estimated Gaussian mixture and has the same number of data points as the real data for comparison with statistical fluctuations. The Q-Q plot shows that the deviations of the experimental data from the mixture of two Gaussians is not larger than the expected deviations due to the finite amount of data.

The Gaussian mixture for the velocities is generated by different flight behavior near a flower versus in open space. This has been verified by splitting the data into flights far from the flower wall vs. flights in the feeding zone. The latter was defined by a cube of side length 9 cm around each flower in which the velocities are determined by approaching a flower and hovering behavior. This separation of different flight phases is thus adapted to accessing the food sources and explains the origin of Gaussian distributions with different variances in both spatial regions. The Lévy flight hypothesis suggests that foraging is characterized by the functional form of such distributions [8, 9]. Surprisingly, by comparing the best fits to these distributions for the different stages of the experiment, we could not detect any differences in the velocity distributions between the spider-free stage and the stages where artificial spider models were present, as is shown in Table II of the Supplemental Material. The parameters of the Gaussian mixture vary between individual bumblebees but there is no systematic change due to the presence of predators.

Hence, we examined the velocity autocorrelation for complete flights from flower to flower. The autocorrelation has been computed by averaging over all bumblebees while weighting with the amount of data available for each time interval; see the Supplemental Material for further details. Figure 3 shows the velocity autocorrelation in the x - and y -directions for different stages of the experiment. In the x -direction (Fig.3(a)) the velocities have no qualitative dependence on the predation risk: They are always anti-correlated for times around 0.5 s, which is due to the tendency of the bumblebees to quickly return to the flower wall. However, the flights with long durations between flower visits become more frequent for stages (2) and (3) compared with stage (1) (inset of Fig.3(a)). This is also reflected quantitatively in a small

shift of the global minimum in the correlations for stages (2) and (3) away from the origin.

An important result is that parallel to the flower wall v_y is anti-correlated in the presence of spiders for $0.7\text{ s} < \tau < 2.8\text{ s}$, while for the spider-free stage it remains positive up to 1.7 s (Fig.3(b)). The vertical z-direction is similar to the y-direction with a weaker dependence on the presence of predators. As the autocorrelation varies between individual bumblebees due to the limited amount of data, we resampled the result by leaving the data of each single bumblebee out (jack-knifing). The resampling (inset of Fig.3(b)) confirms that the differences in the autocorrelation of v_y are due to the presence of spiders.

Our statistical analysis of the experimental data has thus revealed that differences in the foraging behavior of bumblebees, triggered by predation risk, show up in changes of the velocity autocorrelation functions only, and not in modifications of the velocity probability distributions. This is our main result. We emphasize that due to the relatively high density of food sources in our experiment, one may not necessarily have expected to find Lévy-type probability distributions [8]. However, the Lévy paradigm suggests that foraging is fully characterized by such distributions, as was the focus in previous experiments supporting this hypothesis [9–12]. Our results demonstrate that velocity autocorrelation functions contain crucial information for understanding foraging behavior, whereas Lévy flight dynamics are completely uncorrelated and thus predicts them to be trivial.

While we found no changes in the velocity distributions due to the presence of predators, the autocorrelations are consistent with a more careful search: When no threat of predators is present, the bumblebees forage more systematically with more or less direct flights from flower to flower, arching away from the flower wall. Under threat the trajectories become longer and the bumblebees change their direction more often in their search for food sources, rejecting flowers with spiders. This reversing of directions generates the anti-correlations in the y- and z-directions parallel to the flower wall. For the x-direction, the return to the flower wall is responsible for the anti-correlation at small delay times. We did not detect an effect regarding the visibility of the artificial predators with respect to camouflaging. That is, whether the predators were easily visible against the flowers or cryptic made no difference in the estimated distributions and autocorrelations.

These quantities can in turn directly be used for constructing a mathematical model in the form of an overdamped Langevin equation. Our results suggest that the motion of a bumblebee in this experiment obeys the equation

$$\frac{d\mathbf{r}}{dt} = \xi(\mathbf{r}, t)$$

with $\xi(\mathbf{r}, t) = \chi_{fz}(\mathbf{r})\xi_1(t) + (1 - \chi_{fz}(\mathbf{r}))\xi_2(t)$. Here \mathbf{r} is the position of the bumblebee at time t , $\chi_{fz}(\mathbf{r})$ is the characteristic function of the feeding zone, which is equal to one whenever the bumblebee is in the cube around a flower as defined before, and ξ_i , $i = 1, 2$ is Gaussian noise with two different variances σ_i^2 . This sum of two noise terms means that the bees perform a combination of two different flight modes with velocities that

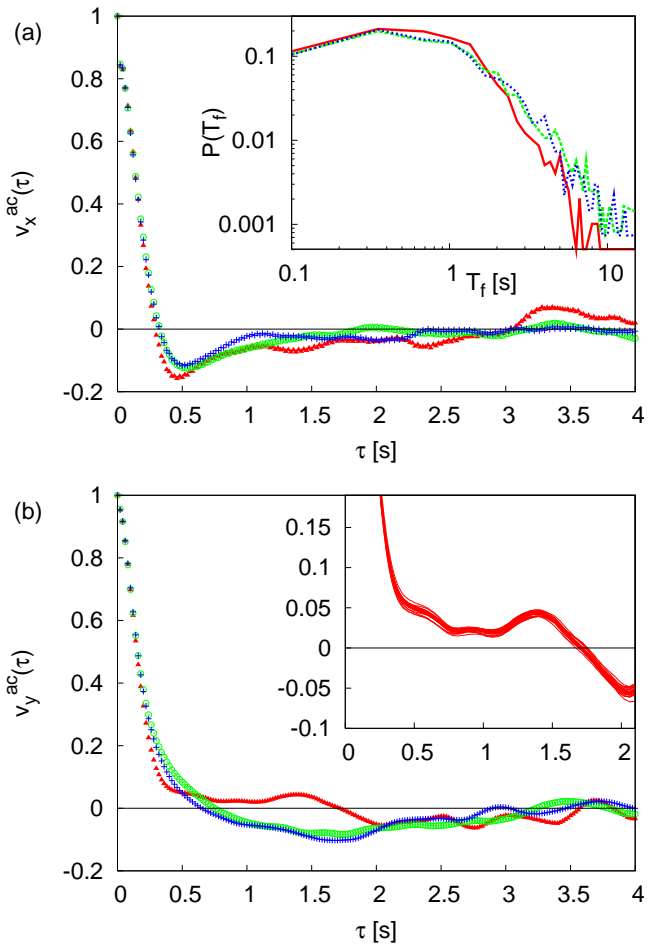


Figure 3. Autocorrelation of the velocities at different experimental stages: without spiders (red triangles), under threat of predation (green circles), and under threat a day after the last encounter with the spiders (blue crosses). (a) In the x-direction the velocities are anti-correlated for small times ($\approx 0.5\text{ s}$) due to short flights from one flower to a nearby flower back at the flower wall. Inset: the distribution of flight-times T_f for each stage shows a corresponding maximum for these short jumps. Under threat of predation (dotted) long flights become more frequent. (b) The correlation of v_y shows the effect of the presence of spiders on the flight behavior of the bumblebees. The inset shows the resampled autocorrelation for the spider-free stage in the region where the correlation differs from the stages with spider models, which confirms that the differences are due to predatory threat.

are different in these two spatial domains. However, the resulting Gaussian process is not a superposition of two ordinary Brownian motions. Our data for the velocity autocorrelations, which determine the correlation decay of $\xi(\mathbf{x}, t)$, show that this motion is strongly non-Markovian with anti-correlations in the velocities. These results suggest a mathematical modeling beyond ordinary correlated random walks, which predict velocity correlations to decay exponentially [28].

The presence of different flight modes and their impact on the velocity distributions show that foraging is governed by different dynamics on different scales of time and space.

Scale-free models such as Lévy flights might thus also be a too simplistic approach to foraging. The motivation for the introduction of Lévy flights into foraging from a theorists' point of view were the existence of a generalized central limit theorem and optimality claims [7, 8], due to being scale-free. It helped further that it is easy to incorrectly identify power laws in log-log-plots [15, 16]. However, in real application in the context of foraging animals, a variety of mechanisms may naturally lead to much more complicated distributions, e.g., individuality of animals [18, 29, 30], an intermittent switching between quasi-ballistic persistent dynamics and localized search modes [6, 17], or quantities over which one has averaged like time of day [12]. As ignoring these mechanisms can lead to spurious power laws, it is important to look for the reasons of the occurrence of non-trivial distributions like mixtures, e.g., animals switching between different search modes. These mixtures may not always be optimal distributions for a particular search problem, but they are easy to produce, composable and flexible enough such that differences to some optimal distribution might not be large enough to give rise to evolutionary pressure [4]. Therefore Lévy flights are probably not a good starting point for the analysis of foraging data even in cases where their optimality holds.

In summary, the fundamental question 'What is the mathematically most efficient search strategy of foraging organisms?' has, under specific conditions [20], been answered by

the Lévy flight hypothesis [7, 8]. This question is well-posed under precise foraging conditions and has the big advantage that it is amenable to mathematical analysis. However, it does not capture the full complexity of a biological foraging problem, which incorporates both the dependence of foraging on 'internal' conditions of a forager (sensory perception [22], memory [21], individuality [18, 29, 30]) as well as 'external' environmental constraints (distribution of food sources [11, 12, 25], day-night cycle [12], predators [26, 27]). Asking about the range of applicability of the Lévy flight hypothesis leads to the over-arching question 'How can we statistically quantify changes in foraging dynamics due to interactions with the environment?', which requires to identify suitable measurable quantities characterizing such changes. This question highlights the need to better understand, and more carefully analyze, the interplay between forager and environment, which would yield crucial information for constructing more general mathematical foraging models.

ACKNOWLEDGMENTS

We thank Holger Kantz for valuable support and Nicholas W. Watkins as well as Michael F. Shlesinger for helpful comments. Financial support by the EPSRC for a small grant within the framework of the QMUL *Bridging The Gap* initiative is gratefully acknowledged.

-
- [1] G. H. Pyke, H. R. Pulliam, and E. L. Charnov, *Q. Rev. Biol.*, **52**, 137 (1977).
 - [2] R. S. Schick *et al.*, *Ecology Letters*, **11**, 1338 (2008).
 - [3] F. Bartumeus, *Oikos*, **118**, 488 (2009).
 - [4] M. G. E. da Luz, A. Grosberg, E. P. Raposo, and G. M. Viswanathan, *J. Phys. A: Math. Theor.*, **42** (2009).
 - [5] P. Smouse *et al.*, *Phil. Trans. R. Soc. B*, 2201 (2010).
 - [6] O. Bénichou, C. Loverdo, M. Moreau, and R. Voituriez, *Rev. Mod. Phys.*, **83**, 81 (2011).
 - [7] M. F. Shlesinger and J. Klafter, *On Growth and Form*, 279 (1985).
 - [8] G. M. Viswanathan *et al.*, *Nature*, **401**, 911 (1999).
 - [9] G. M. Viswanathan *et al.*, *Nature*, **381**, 413 (1996).
 - [10] A. M. Reynolds *et al.*, *Ecology*, **88**, 1955 (2007).
 - [11] D. W. Sims *et al.*, *Nature*, **451**, 1098 (2008).
 - [12] N. E. Humphries *et al.*, *Nature*, **465**, 1066 (2010).
 - [13] M. Lomholt, T. Koren, R. Metzler, and J. Klafter, *Proc. Natl. Acad. Sci. USA*, **105**, 11055 (2008).
 - [14] A. M. Reynolds, *Behav. Ecol. Sociobiol.*, **64**, 19 (2009).
 - [15] A. M. Edwards *et al.*, *Nature*, **449**, 1044 (2007).
 - [16] A. M. Edwards, *J. Anim. Ecol.*, **77**, 1212 (2008).
 - [17] P. Dieterich, R. Klages, R. Preuss, and A. Schwab, *Proc. Natl. Acad. Sci. USA*, **105**, 459 (2008).
 - [18] S. Hapca, J. W. Crawford, and I. M. Young, *J. R. Soc. Interface*, **6**, 111 (2009).
 - [19] D. W. Sims, D. Righton, and J. W. Pitchford, *J. Anim. Ecol.*, **76**, 1365 (2007).
 - [20] A. James, J. W. Pitchford, and M. J. Plank, *Bull. Math. Biol.*, **72**, 896 (2010).
 - [21] J. Burns and J. Thomson, *Behavioral Ecology*, **17**, 48 (2005).
 - [22] J. Spaethe, J. Tautz, and L. Chittka, *Proc. Natl. Acad. Sci. USA*, **98**, 3898 (2001).
 - [23] F. Bartumeus *et al.*, *Proc. Natl. Acad. Sci. USA*, **100**, 12771 (2003).
 - [24] J. M. Morales *et al.*, *Ecology*, **85**, 2436 (2004).
 - [25] E. Kai *et al.*, *Proc. Natl. Acad. Sci. USA*, **106**, 8245 (2009).
 - [26] T. C. Ings and L. Chittka, *Current Biology*, **18**, 1520 (2008).
 - [27] T. C. Ings and L. Chittka, *Proc. R. Soc. B-Biol. Sci.*, **276**, 2031 (2009).
 - [28] F. Bartumeus *et al.*, *J. Theor. Biol.*, **252**, 43 (2008).
 - [29] S. Petrovskii and A. Morozov, *The American Naturalist*, **173**, 278 (2009).
 - [30] C. Hawkes, *J. Anim. Ecol.*, **78**, 894 (2009).

SUPPLEMENTAL MATERIAL

To analyze flights we exclude crawling behavior by removing all data within 1 cm of each platform, leaving from 2000 to 15000 data points (average: 6000) per bumblebee for each stage. We select the best model for the velocity distributions by maximum likelihood estimation and Akaike and Bayesian weights for our candidate distributions [15] for $|v| \geq 2.5$ cm/s. Given a set of measured velocities $D = \{v_1, v_2, \dots, v_n\}$ and a probability density function $\rho_\lambda(v)$, where λ is a vector of k parameters, the *log-likelihood* of the probability density function for a finite resolution of the data ($\Delta v = 5$ cm/s) simplifies to

$$\ln L(\lambda|D) = \sum_{v_j \in D} \ln P_\lambda(v_j) = \sum_{b \in \text{bins}} h[b] \ln \int_{\min(b)}^{\max(b)} \rho_\lambda(v) dv$$

where $h(b)$ is the observed frequency in bin b .

For each candidate distribution $\rho_{\lambda_i}^i$, $i \in \{1, 2, 3\}$, we maximize the log-likelihood $\ln L_i$ w.r.t. λ_i locally with a Nelder-Mead algorithm by using a Monte Carlo method to find the global maximum. To find the preference between the different model distributions whose likelihoods L_i are maximized at λ_i^{\max} the information criteria are

$$IC_i = -2 \ln(L_i(\lambda_i^{\max}|D)) + s(n)k_i$$

with $s(n) = 2$ for the Akaike information criterion and

$s(n) = \ln(n)$ for the Bayesian information criterion as a penalty on the number of parameters k_i . The best model, denoted by $*$, is the one which minimizes the information criterion $IC_* = \min_i(IC_i)$. The Akaike/Bayesian weights then give the preference of each model over the others as a probability

$$w_i = \alpha e^{-(IC_i - IC_*)/2},$$

where α normalizes the weights to $\sum_i w_i = 1$.

The choice of the information criterion makes no strong difference for the model selection in this experiment. With the Akaike information criterion the Gaussian mixture is chosen with a weight of over 95% for all bumblebees and all experimental stages. The Bayesian information criterion agrees with the Akaike information criterion on 90% of all data sets. For the other 10% it prefers a single Gaussian or an exponential distribution - these data sets turned out to be those with the least amount of data available.

To compute the autocorrelation function $v^{ac}(\tau)$ of the flight velocities

$$v^{ac}(\tau) = \frac{\langle (v_t - \mu)(v_{t+\tau} - \mu) \rangle}{\sigma^2}$$

we average over all bumblebees and over time in all flights that are complete from starting on one flower to landing on the next. We exclude flights containing gaps and correlation terms, where in-between time t and $t + \tau$ a flower was visited.

Table I. Model weights and estimated parameters. Akaike and Bayesian weights both give preference to the mixture of two Gaussians for v_y for most of the bumblebees. The weights are estimated individually and their mean and standard deviation (in brackets) are shown. The distribution parameters are also estimated individually for each bumblebee.

Model:	(a) Exponential	(b) Power law	(c) Gaussian	(d) Gaussian Mixture		
Akaike weight	0.00 (0.00)	0.00 (0.00)	0.04 (0.19)	0.96 (0.19)		
Bayesian weight	0.04 (0.18)	0.00 (0.00)	0.08 (0.26)	0.88 (0.30)		
Parameters	λ	μ	σ	a	σ_1	σ_2
average (bumblebees)	5.61	1.11	0.25	0.67	0.06	0.29
stddev (bumblebees)	1.07	0.16	0.03	0.13	0.04	0.03

Table II. Weights and estimated parameters of the Gaussian mixture for the different experimental stages. Weights and parameters are estimated for each bumblebee. Shown are the mean over all individuals and the standard deviation (in brackets). The mixture of two Gaussians is the best fit in all stages. In the parameters of the distribution we observe no significant effect of the threat of predators on the bumblebees.

Stages	Akaike weight	Bayesian weight	a	σ_1	σ_2
(1) Without spiders	0.97 (0.15)	0.93 (0.23)	0.64 (0.11)	0.06 (0.02)	0.29 (0.03)
(2) Under predation risk	0.99 (0.04)	0.90 (0.27)	0.68 (0.13)	0.06 (0.02)	0.29 (0.02)
(3) With risk, 1 day later	0.89 (0.29)	0.80 (0.38)	0.72 (0.16)	0.07 (0.07)	0.30 (0.03)